Noise mechanisms in superconducting tunnel-junction detectors

K. Segall,[a] C. Wilson, L. Frunzio, L. Li, S. Friedrich,[b] M. C. Gaidis,[c] and D. E. Prober[a]
Department of Applied Physics, Yale University, New Haven, Connecticut 06520-8284

A. E. Szymkowiak and S. H. Moseley
NASA Goddard Space Flight Center, Greenbelt, Maryland 20771

(Received 12 November 1999; accepted for publication 4 May 2000)

We present a theory and measurements of noise mechanisms in superconducting tunnel-junction detectors used as single-photon spectrometers. These mechanisms result from incomplete cooling of the excited quasiparticles in the tunnel-junction electrode. Due to the incomplete cooling, only a fraction of the initially created charge is collected by tunneling. Additional effects include reduced dynamic resistance, voltage dependence of the integrated charge, and increased statistical broadening of the signal. We demonstrate these noise mechanisms in our device, and show that they explain the measured energy resolution of 25 eV at 5.9 keV. We also suggest ways to reduce their contribution in future devices. © *2000 American Institute of Physics.* [S0003-6951(00)03526-9]

Superconducting tunnel-junction detectors (STJs) have demonstrated significant promise as nondispersive, photon-counting spectrometers for a broad range of energies, 1–10 eV.[1–4] Applications in astrophysics and materials analysis will benefit from the improved energy resolution, predicted to be 2.8 eV full width at half maximum (FWHM) at 6 keV for absorption in a tantalum superconducting film. This is much better than can be achieved with conventional nondispersive semiconductor detectors ($\approx$120 eV at $E=6$ keV).[5] For visible photons, the ability of the STJ to provide energy resolution for single photons is itself novel.[6] STJs also provide photon timing and high quantum efficiency.

A photon incident on a STJ detector breaks Cooper pairs and creates excess quasiparticles, the number of which is proportional to the energy. The ideal energy resolution of the STJ is limited by the creation statistics of the single-electron excitations (quasiparticles); the FWHM energy resolution is[1]

$$\Delta E = 2.355(F\epsilon E)^{1/2}, \tag{1}$$

where E is the incident photon energy, ϵ is the energy required to create a single excitation, and F is the Fano factor. We assume[1] $\epsilon \approx 1.7\Delta$, where Δ is the energy gap in the superconducting absorber, and[1] $F \approx 0.2$ for Ta, which is better than uncorrelated creation statistics ($F=1$). To date, the energy resolution of STJ detectors above 1 keV is found to be larger than predicted, even when all previously known noise sources[1] are considered. In the range below 1 keV, the theoretical energy resolution is obtained once the known sources of noise are subtracted.[2] However, this is for devices with significant backtunneling, for which[1] $F \approx 1.4$. At higher energies, something is missing in our understanding of the device physics. Guidance on design changes to achieve $F=0.2$ in the visible/UV range may also be needed.

We report here three new noise mechanisms in STJ detectors, all of which result from incomplete thermalization of the quasiparticles prior to tunneling. These include an increase in ΔE due to (1) statistical noise related to the cancellation of the tunneling current caused by reverse tunneling processes, (2) amplifier voltage noise, and (3) bias voltage fluctuations. The last two of these are significant in our devices and, in general, at higher energies (>1 keV). The first is important at all energies. These mechanisms can impose operational limits on performance, e.g., count rate and junction size, which are intrinsic to the device physics. In order to achieve the intrinsic energy resolution, the device designs must achieve better electron cooling.

In recent work, we developed a model for the dynamics and charge collection in our imaging detector.[3] Here, we apply this model to noise considerations. The device consists of a Ta absorber 200 μm long and two Al–oxide–Al tunnel junctions, one at each end of the absorber. The band diagram of one of the junctions is shown in the inset of Fig. 1. A photon, $E \approx 6$ keV, is absorbed in the Ta film and the resulting quasiparticles cool rapidly to the Ta gap energy ($\Delta_{Ta} = 700\,\mu$eV). They then diffuse to the two Al traps, where they enter at an energy Δ_{Ta}, cool toward the Al gap ($\Delta_{Al} = 180\,\mu$eV) by phonon emission, and then tunnel. The integrated excess current is the collected charge, $Q = Ne = \int (I(t) - I_{dc})dt$. The ratio of charge collected in the two traps gives a measure of the position of the photon absorption. The sum of the charges, $Q = Q_1 + Q_2$, provides a measure of the photon energy. We consider below the energy

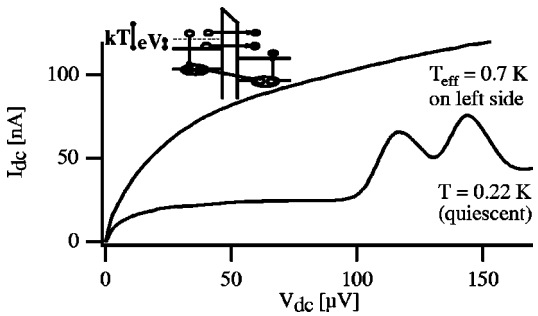

FIG. 1. $I-V$ curve in the quiescent state (bottom) and in the dynamic state (top), with excess quasiparticles in the junction. The Fiske modes in the bottom curve are at $V=120$ and 150 μV; we bias at 70 μV. The top curve is our estimate of the $I-V$ with excess quasiparticles at an energy distribution characterized by $T_{EFF}=0.7$ K. Inset shows possible tunneling processes.

[a]Electronic mail: kenneth.segall@yale.edu; daniel.prober@yale.edu
[b]Current address: LLNL, L-418, P.O. Box 808, Livermore, CA 94550.
[c]Current address: NASA JPL, M/S 168-314, Pasadena, CA 91109.

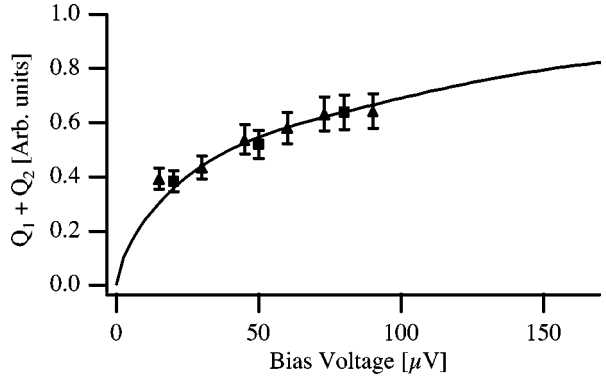

FIG. 2. Total charge Q_1+Q_2 vs bias voltage. The markers are the measured data (from two different cooldowns), the solid line is a fit from a microscopic calculation considering the energy distribution while tunneling.

resolution of the total signal (Q). Where we quote a quantity for a signal junction, that single junction behaves like the two junctions of our detector in parallel.

If all the charge is collected via tunneling, Q is equal to the created charge, $Q_0=eE/\epsilon=eN_0$. We showed previously[3] that the charge collection is incomplete and that the integrated charge depends on the dc bias voltage. As explained below, this incomplete charge collection is due to some of the quasiparticles in the Al traps being at energies $E_{qp}>(\Delta_{Al}+eV_{dc})$. Their energy distribution was computed in a microscopic calculation of the inelastic scattering of quasiparticles as they enter from the Ta absorber. An effective temperature roughly characterizes this distribution. We use the theoretical value of the inelastic scattering parameter for Al, $\tau_0=0.44\,\mu$s.[7] The tunnel time is $\tau_{tun}=2.4\,\mu$s.

In Fig. 1 we show the schematic $I-V$ curves for a STJ for two conditions: (1) the quiescent state, in which the quasiparticles on both sides are in thermal equilibrium at the bath temperature, $T_{bath}=0.22$ K; and (2) shortly after photon absorption, when there are extra quasiparticles on the left side (the trap) at a higher effective temperature, $T_{EFF}=0.7$ K.[8] These quasiparticles have not fully cooled to the gap edge before they tunnel. The number of extra quasiparticles in the trap is taken to be the number produced by the x-ray photon. We bias at $V_{dc}=70\,\mu$V, $kT_{bath}\approx 18\,\mu$eV, and $kT_{EFF}\approx 60\,\mu$eV. For a quasiparticle in the trap at $E_{qp}<(\Delta_{Al}+eV_{dc})$, there is only one tunneling process, transfer of charge to the right (see the inset, Fig. 1). This is the case for almost all thermally excited quasiparticles at our bias voltage and bath temperature. For electrons at $E_{qp}>(\Delta_{Al}+eV_{dc})$ there are two possible processes: direct tunneling to the right, and a pair-mediated process which destroys a pair on the right side and transfers a charge to the left (see the inset, Fig. 1). The pair-mediated process is more likely due to the higher density of final states. For $T_{EFF}=0.7$ K and $V_{dc}=70\,\mu$V, some of the quasiparticles are above the energy $(\Delta_{Al}+eV_{dc})$. Their charge flows on average in the ''backward'' direction and this cancels some of the charge flowing in the ''forward'' direction from quasiparticles at lower energy. Thus, the current and the integrated charge depend on V_{dc}; the initial charge in the Al trap is not fully transferred in the forward direction.[9] We plot in Fig. 2 the experimental data for the integrated charge versus V_{dc}. This compares well to our microscopic calculation of the integrated charge.[3,10] In Fig. 1 note also that the slope of the $I-V$ curve is larger after photon absorption. The idea of incomplete cooling is discussed elsewhere[11] (''balance energy'' is used instead of T_{EFF}), but without computing effects on the noise.

We now consider the implications for device resolution. The previous theory for noise in STJ detectors considered the device electronic characteristics measured without the photon-induced current pulse, took into account only the noise in the signal band, and assumed full charge collection. We find the following when these assumptions are lifted:

$$\Delta E_{tot}^2=\Delta E_{statistics}^2+\Delta E_{current}^2+\Delta E_{bias}^2. \tag{2}$$

We do not find significant spatial broadening in our devices. We believe this is because the lateral diffusion in the Ta prior to trapping averages out small differences between different absorption locations. Devices with vertical trapping structures[2] do exhibit spatial broadening. The statistical broadening, the first term in Eq. (2), is given by Eq. (1) only when the full created charge eN_0 is collected via tunneling.

A new statistical noise mechanism arises from the canceling currents. The occurrence of the pair-mediated reverse process (Fig. 1, inset) has two effects: it annihilates a quasiparticle from the trap so that the quasiparticle cannot tunnel to the right and it transfers a charge in the reverse direction, thus subtracting a charge $2e$ from the total charge which might be expected. If there are γN_0 reverse tunneling events, the net charge is then $Q=eN_0(1-2\gamma)$. The γN_0 quasiparticles are chosen randomly from the initial N_0 with its associated statistical uncertainty. This uncertainty can dominate the creation statistics. We find the energy width due to creation statistics and cancellation is

$$\Delta E_{statistics}=2.355\left(\frac{4\gamma(1-\gamma)}{(1-2\gamma)^2}+F\right)^{1/2}(\epsilon E)^{1/2}. \tag{3}$$

Here, $F=0.2$. This expression does not include contributions from quasiparticle recombination, charge multiplication upon trapping, or backtunneling.[10] Equation (3) is derived by assuming a binomial distribution for the number of quasiparticles that undergo the reverse tunneling process. As γ increases this expression can significantly exceed that given by Eq. (1). Typical values for γ are 0.1–0.2; if γ approaches 0.5 the expression in Eq. (3) diverges because the signal (Q) goes to zero. Note that the transfer of a charge in the reverse direction makes the noise different than absorber loss, which only prevents a quasiparticle from tunneling. We discuss detailed dependence on device parameters and the additional statistical noise terms in a future paper.[10]

The second term in Eq. (2) is from current noise in the signal band, which is integrated along with the signal current, and thus causes variation of the integrated charge. The current noise spectral density in the signal frequency band is

$$\Delta E_{Current}^2\propto I_{TOT}^2=(I_{Shot}^2)+(I_{Johnson}^2)+(e_{TOT}^2/R_{EFF}^2). \tag{4}$$

Here, e_{TOT}^2 is the total voltage noise spectral density in the signal band; usually, $e_{TOT}^2=e_A^2$, with e_A due to the amplifier. The shot-noise term $2eI_{dc}$ and the Johnson noise term $4kT/R_f$, due to the feedback resistor, are the standard terms.[12] However, the last term—current noise resulting from the total voltage noise—is different in that R_{EFF} is the resistance during the pulse, not that in the quiescent state.

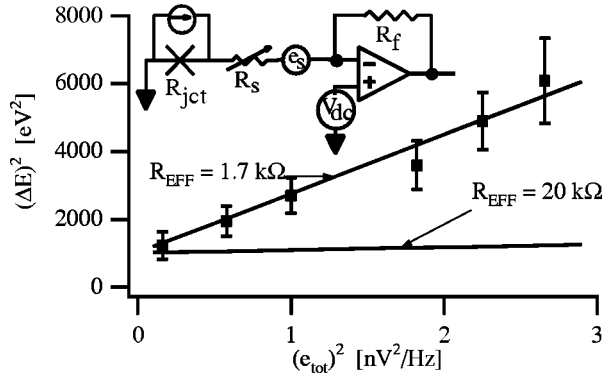

FIG. 3. Energy resolution squared vs total voltage noise squared. A best fit is obtained for $R_{\mathrm{EFF}}=1.7\,\mathrm{k}\Omega$, instead of the 20 kΩ in the quiescent state. See Ref. 12 for calibration measurements. The inset shows a schematic of the circuit, with R_s the series resistor providing the excess voltage noise.

The last term in Eq. (2) accounts for fluctuations in the bias voltage that cause the integrated charge to vary from one pulse to the next. In our case, this fluctuation is caused by the low-frequency noise of our dc-coupled, wideband amplifier. This noise is outside of our signal band and causes qualitatively different noise behavior than the in-band noise. This problem can be reduced by ac coupling the amplifier.

Two of the new noise sources, due to the reduced value of R_{EFF} and due to low-frequency bias voltage fluctuations, can be quantitatively demonstrated in our devices. First consider R_{EFF}. We determined R_{EFF} by physically adding to the in-band amplifier voltage noise e_A an extra known noise voltage e_S due to the Johnson voltage noise of a series resistor at room temperature. We measured the increase in the energy width $\Delta E_{\mathrm{TOT}}^2$ as a function of $e_{\mathrm{TOT}}^2=e_A^2+e_S^2$. The data are shown in Fig. 3. We have accounted for the minor change in the current pulse due to this added series resistance. The slope of the curve gives $R_{\mathrm{EFF}}=1.7\,\mathrm{k}\Omega$.[12] This is much smaller than $dV_{\mathrm{dc}}/dI_{\mathrm{dc}}$ of the quiescent state, ≈20 kΩ. This predicts $\Delta E=16\pm3$ eV due to the last term in Eq. (3).

To investigate the effect of bias voltage fluctuations, we measured the variation of the dc voltage across the junction under typical operating conditions in the quiescent state. We sampled the device voltage at the same rate and for a similar time period as when x rays are detected. With our existing amplifier the measured voltage variation due to $1/f$ voltage noise is $\Delta V=0.35\pm0.07\,\mu$VFWHM. This leads to an energy width $\Delta E_{\mathrm{bias}}=(E/Q)(dQ/dV)\,\Delta V=11\pm2$ eV.

The energy widths due to these two noise mechanisms scale linearly with the energy, $\Delta E\propto E$, and are thus more significant at large photon energies than the energy width of Eq. (1). The magnitude of these mechanisms has not typically been significant for $E<1$ keV in devices studied to date. However, at $E=6$ keV, the magnitude of each of these two terms can be comparable to the total of all other noise mechanisms. This is shown in Table I. Including these terms, we find that the predicted energy width matches well with the experimental[4] total. Future data over a range of parameters should verify the scaling of these noise terms.

To reduce the magnitude of the noise sources we have identified, one should make an effort to improve the electron cooling. The main approaches are to lengthen the tunnel time and to bias at a larger dc voltage. The latter is not straightforward in our present devices due to the presence of Fiske modes (Fig. 1). A cold feedback resistor, a lower operating temperature to reduce the shot noise, and an ac coupled amplifier are also desirable. These improvements predict an energy resolution[13] of 5.1 eV (Table I), close to the intrinsic broadening of Eq. (1). These considerations also provide guidance for using materials with different scattering times.[10]

TABLE I. Energy resolution at 5.89 keV for the present device and for a projected one. The projected device has $V_{\mathrm{dc}}=160\,\mu$V, $T_{\mathrm{bath}}=0.1$ K, a tunnel time $\tau_{\mathrm{tun}}=12\,\mu$s, a cold feedback resistor, and an ac coupled amplifier. The statistical width includes additional terms (see Ref. 13), which are not in Eq. (3), from backtunneling, trapping multiplication, and recombination. Bold numbers include contributions from the noise sources.

Noise mechanism	Present ΔE (eV)	Projected ΔE (eV)
Statistical width [Eq. (3) and other terms]	**8.7**	4.7
Current noise: shot noise [Eq.(4)]	7.2	0.6
Current noise: Johnson [Eq. (4)]	9.4	0.6
Amplifier voltage noise [Eq. (4)]	**16.0**	1.8
Bias voltage fluctuations [Eq. (2)]	**11.0**	0.6
ΔE_{TOT} (predicted)	24.3	5.1
ΔE_{TOT}	25.4	···

The authors thank P. J. Kindlmann, R. G. Wheeler, D. Schiminovich, and R. Shoelkopf for useful discussions. This work was supported by NASA Grant No. NAG5-2892 and NASA Fellowships for K.S., M.G., and C.W.

[1] N. Booth and D. J. Goldie, Supercond. Sci. Technol. **9**, 493 (1996); for the Fano factor and ϵ for Sn, see M. Kurakado, Nucl. Instrum. Methods Phys. Res. A **196**, 275 (1982); for Nb, see N. Rando, A. Peacock, A. van Dordrecht, C. Foden, R. Engelhardt, B. G. Taylor, and P. Gare, *ibid.* **313**, 173 (1992); we assume Ta to be similar to these two metals.

[2] P. Verhoeve, N. Rando, A. Peacock, A. van Dordrecht, B. G. Taylor, and D. J. Goldie, Appl. Phys. Lett. **72**, 3359 (1998); P. Verhoeve, N. Rando, A. Peacock, A. van Dordrecht, and A. Poelaert, IEEE Trans. Appl. Supercond. **7**, 3359 (1997); J. B. le Grand, C. A. Mears, L. J. Hiller, M. Frank, S. E. Labov, H. Netel, D. Chow, S. Friedrich, M. A. Lindeman, and A. T. Barfknecht, Appl. Phys. Lett. **73**, 1295 (1998).

[3] S. Friedrich, K. Segall, M. C. Gaidis, C. M. Wilson, D. E. Prober, A. E. Szymkowiak, and S. H. Moseley, Appl. Phys. Lett. **71**, 3901 (1997).

[4] K. Segall, C. M. Wilson, L. Li, A. K. Davies, R. Lathrop, M. C. Gaidis, D. E. Prober, A. E. Szymkowiak, and S. H. Moseley, IEEE Trans. Appl. Supercond. **9**, 3226 (1999).

[5] R. C. Alig, S. Bloom, and C. W. Struck, Phys. Rev. B **22**, 5565 (1980).

[6] Transition-edge superconductor detectors can also provide single-photon energy resolution in the UV/visible of the same order as the STJs.

[7] S. B. Kaplan, C. C. Chi, D. N. Langenberg, J. J. Chang, S. Jafarey, and D. J. Scalapino, Phys. Rev. B **14**, 4854 (1976).

[8] The energy distribution of the created quasiparticles in the trap is roughly characterized by T_{EFF}. The number of created quasiparticles is small, so the energy gap is determined by T_{batt}.

[9] We have considered only processes which originate from the trap. The cancellation of processes from the counterelectrode (backtunneling and reverse tunneling) also contributes a small voltage dependence.

[10] K. Segall, Ph.D. thesis, Yale University; K. Segall *et al.* (unpublished).

[11] A. Poelaert, A. Kozorezov, A. Peacock, K. Wigmore, P. Verhoeve, A. van Dordrecht, A. Owens, and N. Rando, Proc. SPIE **3445**, 214 (1998).

[12] The amplifier voltage noise is $0.4\,\mathrm{nV/(Hz)^{1/2}}$ in the signal band; the in-band current noise of the feedback resistor and shot noise together are $0.17\,\mathrm{pA/(Hz)^{1/2}}$. We use conversion factors of $72\,\mathrm{eV/(pA/(Hz)^{1/2})}$ and $42\,\mathrm{eV/(nV/(Hz)^{1/2})}$ for voltage and current noise, respectively.

[13] The statistical noise due to Eq. (3) is 5.0 eV for the present device and 2.8 eV in the projected device. The remaining statistical noise from backtunneling, absorber loss, and multiplication upon trapping is 7.1 eV in the present device and 3.8 eV in the projected one; see Ref. 10.